Title: Rapid decline in Western monarch butterflies leads to phenological and geographic Allee effects

Authors: Collin Edwards[12]*, Cheryl Schultz[2], Elizabeth Crone[1]

Affiliations:

[1]Department of Biology, Tufts University; Somerville, MA

[2]School of Biological Sciences, Washington State University; Vancouver, WA

*Corresponding author. Email: edwards.evoeco@gmail.com

Summary: Allee effects are processes that become disrupted at low population sizes, causing further declines to eventual extinction (1, 2). Identifying Allee effects in natural populations is important for both ecological theory and conservation efforts, but challenging because populations typically only experience them briefly before collapsing (3, 4). In 2018, the Western monarch butterfly population fell below the threshold that scientists predicted would trigger Allee effects (5). Here we show that since 2018, the Western monarch population has expanded more slowly during spring and summer breeding and filled a smaller breeding range. Other aspects of the monarch life cycle (winter survival, fecundity, morphology) have not declined after the crash. However, winter survival is much lower and wing sizes of overwintering monarchs are larger now than in the 20th century, suggesting higher mortality and selection for increased dispersal in recent decades. Delayed arrival to parts of the Western monarch breeding range is a

novel Allee effect, which could lead to temporal mismatches between monarchs and their and host plants. We do not know whether this change will contribute to future declines. However, we do know that we should expect surprising changes in processes as populations reach unprecedentedly low sizes.

When populations decline to very low densities, individuals can face additional distinct challenges, such as difficulty finding mates, that decrease population growth (*1*). These challenges can cause even more rapid declines, possibly contributing to an extinction vortex (*2)*. Positive density dependence at low population size – known as Allee effects – can drive prevent invasions as well as driving extinctions (*3)*. Documenting and understanding Allee effects is important both for conservation biology and for broader ecological theory. However, observations of Allee effects in nature are rare. Because Allee effects lead to further population decline, there is only a very narrow window of time when Allee effects are observable before a population is extirpated (*4)*.

Western monarch butterflies have rapidly declined in the past forty years (Fig 1). Overwintering population estimates were millions of butterflies in the 20th century, but the population declined by an average of 6% per year through 2016 (*5)*. Causes of these declines include agricultural intensification, loss of breeding and overwintering sites (many of which are not protected) (*6)*, and climate (*7)*. In 2017 we predicted that Allee effects would occur if the Western monarch population fell below 30,000 overwintering individuals (*5)*. The following season there was a massive decline, and the population dipped below that threshold at Thanksgiving 2018 (27,721 overwintering individuals) (*8)*. During the next two years, as predicted, the population declined even more dramatically. In Thanksgiving 2020, there were only 1,914 overwintering individuals.

Following the Thanksgiving 2018 crash, we measured demographic processes that could contribute to Allee effects (*9)* (Fig. 1B, Methods). We compared these measures to previously published estimates, categorizing data into three eras: “historical”, before 2000 when there were millions of monarchs; “recent past”, from 2000-2017 when monarchs were in the hundreds of

thousands; and “current”, from 2018-2020 when winter counts were below the hypothesized threshold for Allee effects (Fig. 1A). Differences between the current era and recent past indicate Allee effects. Differences between the historic era and current or recent past indicate possible drivers of long-term declines.

There were no Allee effects in overwinter survival (Fig. 2A), body mass (Fig. 2B), wing length (Fig. 2C), or mating success (Fig. 2D) (see also Supplementary Text). In contrast, there were strong Allee effects in breeding season range. The historic and recent past eras had similar breeding range dynamics (Fig. 3B), with the 0.9 quantile of the population expanding to up to 1070 and 1003 kilometers from overwintering sites, respectively (Fig. 2F). The 0.9 quantile represents the boundary between the 10% of monarchs that are most distant and the remaining 90%, and acts a measure of breeding season range size that is robust to outliers. Since the population dropped from ~167,000 to below 30,000, this maximum distance traveled fell by more than 50%, to 491 kilometers. Western monarch butterflies also experienced a shorter breeding season in the current era, with summer population expansion stopping almost a week earlier (Fig. 3C). Further, in the current era, monarchs have reached regions within their extant breeding grounds up to two months later (Fig 3D,E).

Across ecological systems, shifts in phenology are one of the most conspicuous effects of climate change (*10)*. These shifts can lead to temporal mismatches between interacting species, including insects and their hosts or nectar sources (*11)*. The shift in monarch butterfly phenology reported here differs dramatically from typical climate responses; the average phenological shift across 203 species in the Northern hemisphere is 2.8 days per decade (*10)*, while between recent past and current eras, monarch arrival times were delayed between 3.6 and 60.2 days, depending on distance from overwintering sites. Given the general shift of plant leaf out occurring earlier in

recent years in response to climate change (*12)*, our findings suggest that later generations of monarch butterflies are now experiencing very different life stages ("phenophases") of both their milkweed hostplants and their nectar sources. This shift is especially concerning because monarch caterpillar survival and growth depend strongly on their phenology in relation to host plants and predators (*13)*.

Although not Allee effects, there were two notable changes between the historic and current eras: a reduction in overwintering survival (Fig. 2A), and an increase in body size and particularly wing length (Fig. 2B and C). Reduced winter survival may have contributed to the long-term decline of the Western monarch butterfly. This could reflect reduced overwintering habitat quality or climate-change disruption of overwintering behavior (*14)*, or factors reducing butterfly conditions in the summer breeding ground (*7)*. Larger body size and wing length (measured in February) may indicate biased overwintering survival, with smaller individuals dying at high rates through the winter. Alternately, monarchs may have experienced strong selection for higher movement capabilities across the last few decades. (*15)* hypothesized that the Central Valley of California (immediately east of many overwintering sites) has been substantially degraded as monarch butterfly habitat, and detected pesticides on all milkweeds sampled there. If selection favored individuals that flew past the Central Valley, populations may have evolved increased wing size, which is associated with long-range movement in monarchs (*16)*.

The Allee effects we found were not the ones we expected (*5)*, highlighting the ways in which dynamics become surprising in small populations. Similarly, while finalizing this manuscript, early reports indicate there will likely be 50,000 or more individuals in the 2021 Thanksgiving count, far more than in 2020, but still much less than the counts prior to 2018.

Preliminary analyses suggest that the western monarch breeding range in the summer of 2021 was not a return to the fast expansion and larger breeding range of the recent past or historic eras (Extended Data Fig. 3). Instead, the population increased this year *in spite of* reduced breeding season range. This recent change highlights that we do not know whether reduced colonization of the breeding range is a cause of population declines, or simply a consequence of unprecedentedly low population sizes. As populations approach extinction, population growth rates of many animal species become more variable among years (*17)*. One important lesson from all aspects of this system is that we should expect surprises in population dynamics, as species enter uncharted conditions. It is easy to understand uncharted conditions in terms of the external environment, but it is equally important to recognize the importance of how populations respond to changes in their own abundance, and unprecedentedly low – or, in other systems high – population sizes.

Reference

1. P. A. Stephens, W. J. Sutherland, R. P. Freckleton, What is the Allee effect? Oikos, 185–190 (1999). doi: 10.2307/3547011

2. M.E. Gilpin & M.E. Soulé, M.E. (1986). Minimum viable populations: processes of extinction. In: *Conservation Biology: The Science of Scarcity and Diversity* (ed. Soulé, M.E.). Sinauer Associates, Sunderland, MA, pp. 19–34.

3. F. Courchamp, T. Clutton-Brock, B. Grenfell, Inverse density dependence and the Allee effect. Trends Ecol. Evol. 14, 405–410 (1999). doi: 10.1016/S0169-5347(99)01683-3

4. M. Kuussaari, I. Saccheri, M. Camara, I. Hanski, Allee Effect and Population Dynamics in the Glanville Fritillary Butterfly. Oikos. 82, 384–392 (1998). doi: 10.2307/3546980

5. C. B. Schultz, L. M. Brown, E. Pelton, E. E. Crone, Citizen science monitoring demonstrates dramatic declines of monarch butterflies in Western North America. Biol. Conserv. 214, 343–346 (2017). doi: 10.1016/j.biocon.2017.08.019

6. E. M. Pelton, C. B. Schultz, S. J. Jepsen, S. H. Black, E. E. Crone, Western Monarch Population Plummets: Status, Probable Causes, and Recommended Conservation Actions. Frontiers in Ecology and Evolution. 7, 258 (2019). doi: 10.3389/fevo.2019.00258

7. E. E. Crone, E. M. Pelton, L. M. Brown, C. C. Thomas, C. B. Schultz, Why are monarch butterflies declining in the West? Understanding the importance of multiple correlated drivers. Ecol. Appl. 29 (2019). doi: 10.1002/eap.1975

8. Xerces Society. Western Monarch Thanksgiving Count Data, 1997– 2020. Available at www.westernmonarchcount.org Accessed 23 January 2021. (2021)

9. P. A. Stephens, W. J. Sutherland, Consequences of the Allee effect for behaviour, ecology and conservation. Trends Ecol. Evol. 14, 401–405 (1999). doi: 10.1016/S0169-5347(99)01684-5

10. P. C. Parmesan, Influences of species, latitudes and methodologies on estimates of phenological response to global warming. Glob. Chang. Biol. 13, 1860–1872 (2007). doi: 10.1111/j.1365-2486.2007.01404.x

11. J. R. Forrest, Complex responses of insect phenology to climate change. Curr Opin Insect Sci. 17, 49–54 (2016). doi: 10.1016/j.cois.2016.07.002

12. S. Piao, Q. Liu, A. Chen, I. A. Janssens, Y. Fu, J. Dai, L. Liu, X. Lian, M. Shen, X. Zhu, Plant phenology and global climate change: Current progresses and challenges. Glob. Chang. Biol. 25, 1922–1940 (2019). doi: 10.1111/gcb.14619

13. L. H. Yang, M. L. Cenzer, Seasonal windows of opportunity in milkweed-monarch interactions. Ecology. 101, e02880 (2020). doi: 10.1002/ecy.2880

14. J. S. Bale, S. A. L. Hayward, Insect overwintering in a changing climate. J. Exp. Biol. 213, 980–994 (2010). doi: 10.1242/jeb.037911

15. C. A. Halsch, A. Code, S. M. Hoyle, J. A. Fordyce, N. Baert, M. L. Forister, Pesticide contamination of milkweeds across the agricultural, urban, and open spaces of low-elevation Northern California. Frontiers in Ecology and Evolution. 8, 162 (2020). doi: 10.3389/fevo.2020.00162

16. L. H. Yang, D. Ostrovsky, M. C. Rogers, J. M. Welker, Intra-population variation in the natal origins and wing morphology of overwintering Western monarch butterflies *Danaus plexippus*. Ecography . 39, 998–1007 (2016). doi: 10.1111/ecog.01994

17. W. F. Fagan, E. E. Holmes, Quantifying the extinction vortex. Ecol. Lett. 9, 51–60 (2006). doi: 10.1111/j.1461-0248.2005.00845.x

18. J. M. Calabrese, W. F. Fagan, Lost in time, lonely, and single: reproductive asynchrony and the Allee effect. Am. Nat. 164, 25–37 (2004). doi: 10.1086/421443

19. L. Avilés, P. Tufiño, Colony size and individual fitness in the social spider Anelosimus eximius. Am. Nat. 152, 403–418 (1998). doi: 10.1086/286178

20. R. F. Denno, M. A. Peterson, Density-dependent dispersal and its consequences for population dynamics. Population dynamics: new approaches and synthesis, 113–130 (1995).

21. M. E. Payton, M. H. Greenstone, N. Schenker, Overlapping confidence intervals or standard error intervals: what do they mean in terms of statistical significance? J. Insect Sci. 3, 34 (2003). doi: 10.1093/jis/3.1.34

22. GBIF.org. 17 December 2020. GBIF Occurrence Download doi: 10.15468/dl.aq6d3w

23. Western Monarch and Milkweed Occurrence Database. 2018. Data accessed from the Western Monarch Milkweed Mapper, a project by the Xerces Society, U.S. Fish and Wildlife Service, Idaho department of Fish and Game, www.monarchmilkweedmapper.org. Accessed: 12/3/20.

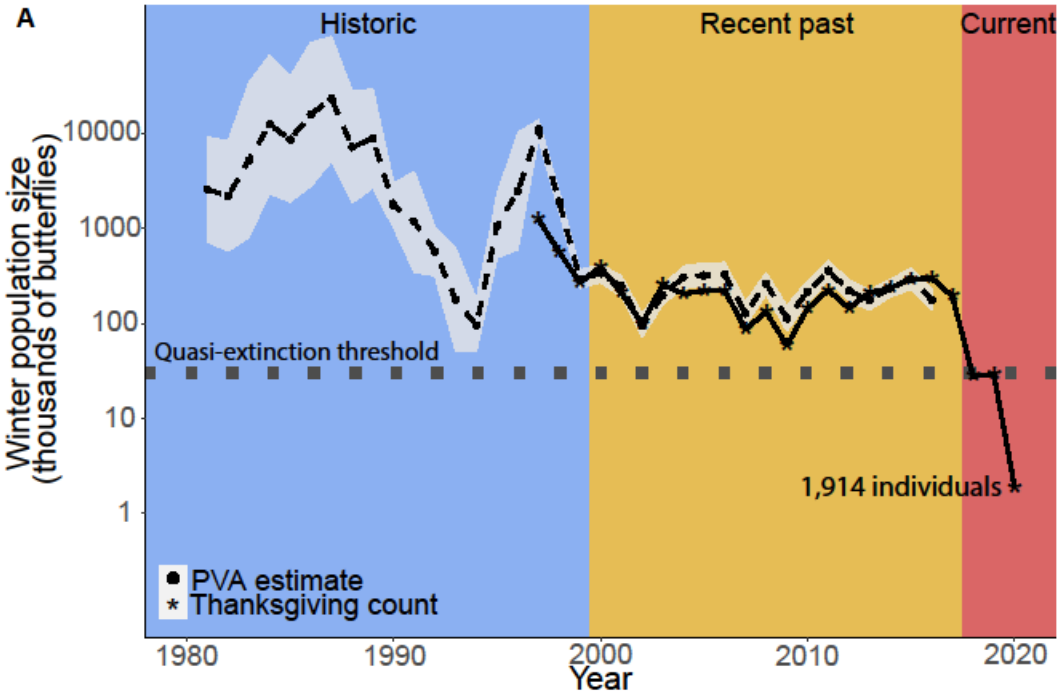

B

Hypothesized component Allee effect	Examples	Monarch performance metric tested	Allee effect
Reduced mating success	(*16*)	% mated	*none*
		eggs per day	*none*
Reduced group facilitation	(*17*)	winter survival	*none*
		body mass	*none*
		wing length	*none*
Density dependent movement	(*3, 18*)	maximum range	~50% reduced breeding season range
		phenology	Massive delays scaling with distance from overwintering sites

Fig. 1. Western monarch populations have collapsed, and Allee effects may disrupt their life cycle and breeding season range. (**A**) Monarch populations have fallen dramatically from the 1900s to today; in winter 2017/2018 populations fell below the hypothesized Allee effect threshold. Estimated population abundances using MARSS state-space model (dashed) and Xerces Thanksgiving counts (solid); note log scale. Plot colored by eras used in analyses. (**B**) Summary of hypotheses behind Allee effects tested in this study, and our conclusions based on data for Western monarch butterflies (see Fig. 2).

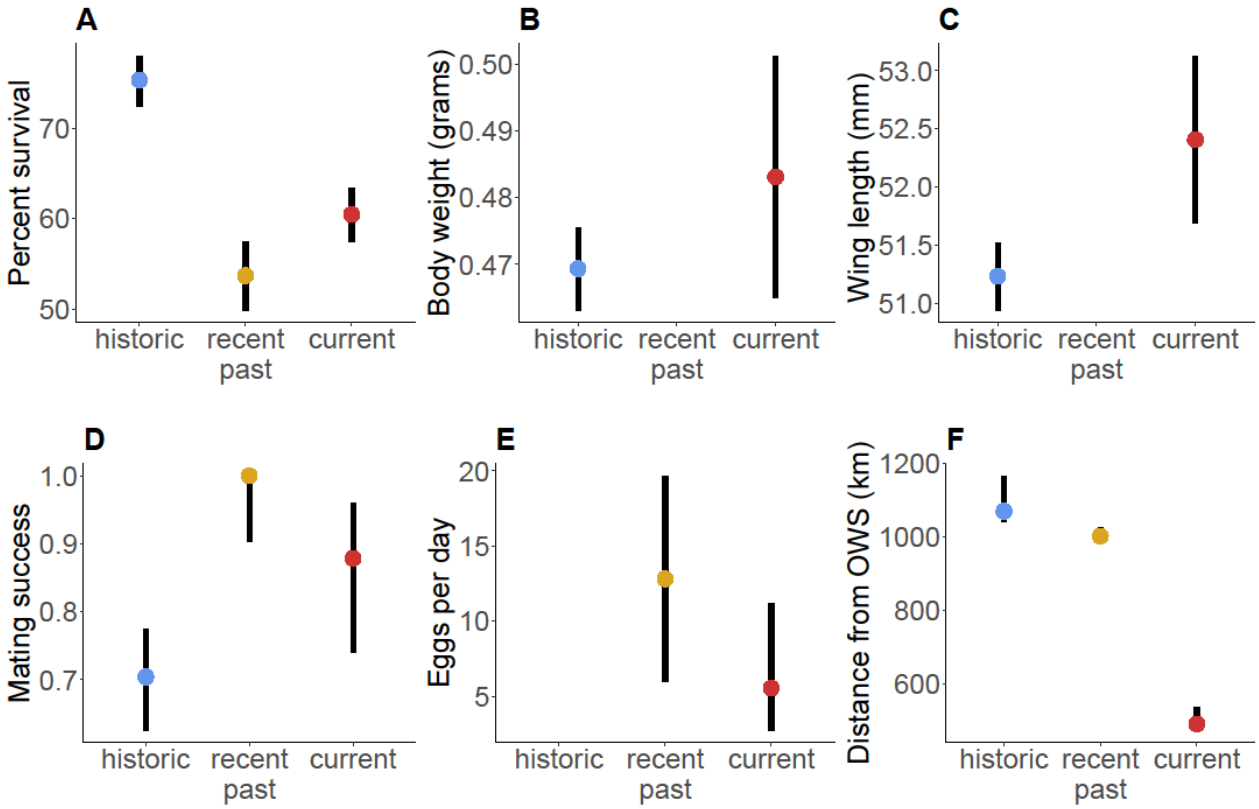

Fig. 2. Alle effects evaluated in Western Monarchs. Comparison across eras for (**A**) winter survival (from Thanksgiving to New Year's Day), (**B**) body mass, (**C**) wing length, (**D**) mating success as measured by proportion of females mated, (**E**) fecundity, and (**F**) breeding season range as measured by maximum distance from overwintering sites. Points correspond to estimated values before 2000 ("historic"), from 2001-2017 ("recent past"), and from 2018-2020 ("current") when the population has been below the hypothesized Allee effect threshold. In some cases (B, C, E), there were no published data available to compare with one of either the historic or recent past eras. Bars represent 84% confidence intervals (nonoverlapping bars represent significant differences) (*21)*. Allee effects imply a decrease in performance for very small populations; for the Western monarch butterfly, this means a change from the recent past to the current era. Only breeding season range (F) shows signs of an Allee effect.

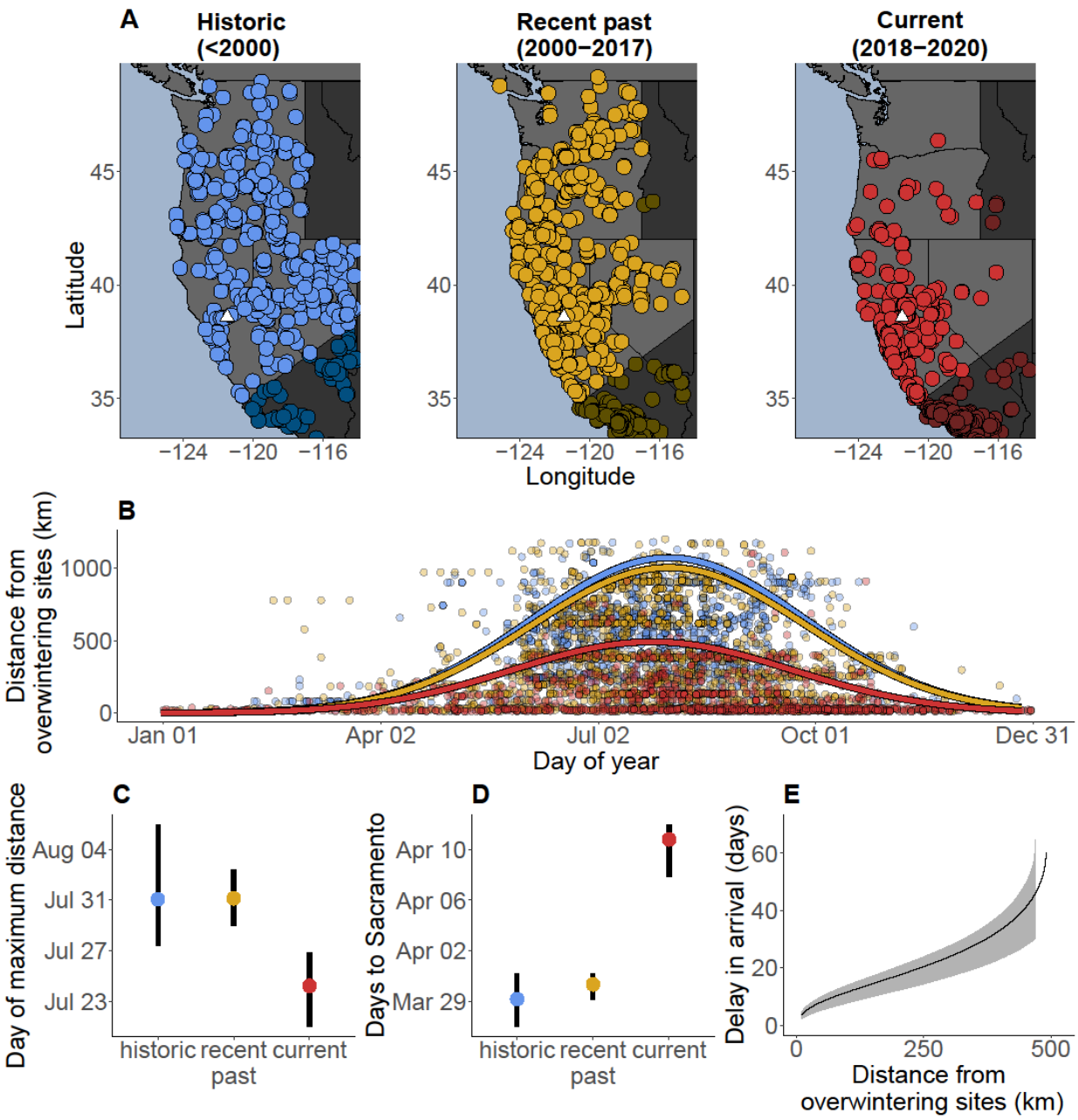

Fig. 3. Breeding season range expansion has shifted dramatically since the monarch population fell below the hypothesized Allee effect threshold. (**A**) observations from iNaturalist (*22)* and the Western Monarch Milkweed Mapper (*23)* through August 1 show fewer observations in OR and WA in the current era. Shaded southern CA and NV excluded to avoid resident populations. White triangles show Sacramento, CA (see D). (**B**) Fitted curves of the 0.9

quantile of the distance from observations to the nearest overwintering site (a measure of expansion into the summer breeding range) show similar patterns between historic era and recent past, but substantial reduction in the current era. (**C**) Comparisons across eras of day of the maximum distance (ie day of peak in (B)) show monarchs now leave their summer breeding range sooner. (**D**) Days for the 0.9 quantile to reach 100 km from the nearest overwintering site, corresponding to the time monarchs would first reach Sacramento, CA; arrival day is much later in current era than in recent past or historical era. (**E**) Phenology in the current era is delayed compared to the recent past, with more delay further from overwintering sites. Black line: difference in arrival of 0.9 quantile in current era compared to recent past. In C&D, bars show 84% confidence intervals calculated via bootstrapping; in E, gray region shows 95% CI.

Methods:

All analysis were carried out in the programming language R version 4.0.2 (*24)*, and the analysis scripts are available as supplements.

Monarch population size

We present estimates of monarch overwintering population size from 1981-2016 using published estimates from state-space (MARSS) models (*5e, 25)*. State space models are not good at estimating rapid changes in population abundance until several years after the change in size. This limitation is because state space models require data after a population crash to estimate whether declines are real or due to a reduction in sampling effort and detection probability. In fact, sites were probably searched more thoroughly after the crash, which would make estimates biased to be too high, not too low. Therefore, we present absolute abundance estimates from Xerces Society Thanksgiving Counts (*8)* from 1997-2020 to illustrate trends in recent years.

Extracting and combining published results

To obtain estimates for monarch performance from past studies, where possible we used raw data from published tables and carried out our own analyses as described below. Where this was not possible, we extracted means and standard deviations from published figures using WebPlotDigitizer (*26)*. When more than one data set was available for the same era, we combined the estimates using the delta method (*27)* as implemented by the deltamethod() function in the R package **msm** (*28)*. The delta method is a flexible mathematical tool for estimating the variance of a derived parameter estimate (e.g. the average of two or more parameter estimates, each with their own variance).

Winter Survival

We used changes in the number of monarch butterflies at overwintering sites to estimate winter survival. Starting in January 2017 (winter 2016-17), the Xerces' Society started organizing surveys in early January ("New Years Count" data) to complement their Thanksgiving Count data (*8)*. We used binomial regression to estimate winter survival for this period as the ratio of the summed New Year's Count (events) to the Thanksgiving Count (trials) for each year from winter 2016-2017 through winter 2020-2021. We fit these five years of data in a single binomial regression model, with a fixed effect of era ("recent past" for the first two winters, and "current" for the most recent three) and a random effect of year. Point estimates of survival for each year support the lack of Allee effects in these data, in the sense that no years in the "current" era had lower survival than the "recent past" (Extended Data Fig. 1).

To estimate survival in the "historic" era, we used analyses presented by (*6)*. This previous analysis used mark recapture data presented in (*30)* to estimate 6-week survival for Western monarchs in 1975-1976 near Santa Cruz and Santa Barbara (6 weeks is approximately the time between the Thanksgiving and New Years Counts). For this paper, we combined the survival estimates for the two locations using the delta method. For this analysis, we corrected one typo in the (*6)*: the "29% drop" for Santa Cruz should instead say "19% drop".

Early spring morphology and reproduction

In February 2019, we collected 35 individual female butterflies from Pismo Beach State Park. We measured body mass and wing length of these individuals. For both measures of body size, we estimated means and standard errors using 0-intercept regression models. For comparison to current body size, we digitized means and standard errors of body mass data for female western monarchs from (*31)* (data from February 1972) and (*32)* (data from February in years 1990-1992). We combined these measures using the delta method. For comparison to

historic wing size, we digitized data from (*33)*, (*30)*, and (*32)*, who reported estimates for wing length of female Western monarchs caught in Februaries 1938-1939 and 1942 , February 1976, and Februaries 1990-1992 respectively. We combined these measures using the delta method.

We used the monarch spermatophore palpation method to evaluate whether butterflies collected in 2019 had been mated (*34)*. We treated any female with a palpation score of 1 ("rice grain or large pinhead") or higher as having successfully mated, and scores of 0 as unmated. Two individuals had an uncertain score and were excluded from further analysis. We used an intercept-only binomial regression model to estimate proportion of mated individuals in the Pismo Beach data. (*32)* caught 142 females in February of 1990, 1991, and 1992, and identified mating status using dissections and spermatophore identification; (*35)* did the same with 19 females caught in February 2010. In both cases we fit the data with the same model structure as our Pismo data.

To estimate daily fecundity, we kept female monarchs from Pismo Beach in tents in the greenhouse for two days with access to milkweed plants (*Asclepias fascicularis*) and nectar plants. At the end of two days, we counted all eggs laid by each female during this time and released butterflies back into the site from which they were collected. We analyzed these oviposition data using 0-inflated negative binomial models (using the **pscl** package in R) (*36e, 37)*, a statistical technique that separates 0's (in this case, butterflies that were not reproductively active) from a process that might include 0's and higher values (in this case, eggs laid per day for butterflies that are reproductively active). The models produce two parameters: the proportion of 0's (hereafter, the proportion of non-reproductive butterflies), and the mean of the non-zero distribution (here, the average count of eggs per reproductive butterfly). We used the mean of the non-zero distribution divided by two as our estimated eggs laid per day. We compared these

values to data from (*35)*. They provide estimated means and standard deviations for the lifespan (N=19) and lifetime eggs per female (N=10) for monarchs in February 2010. We calculated mean eggs per day as mean lifetime eggs divided by mean lifespan and used the delta method to estimate the associated standard error.

(35) carried out manipulations specifically to break female monarchs from reproductive diapause. We did not manipulate environmental conditions to break diapause to minimize impacts on wild populations during this critical time. Therefore, 0's from the 0-inflated negative binomial models likely represent butterflies in reproductive diapause, but could also represent unmated butterflies. We do not interpret these data further.

Breeding season range

The Western monarch butterfly has a multi-generational life cycle: overwintering individuals emerge from dormancy and travel from the coast of California to lay eggs before they die; many of their offspring also fly substantial distances before laying eggs, and across 3-4 generations each summer the butterflies spread throughout the western United States and into very southern Canada (*38)*. The final generation flies back to overwintering sites on the coast of California in the fall, completing the cycle.

We obtained observations of monarchs in California, Oregon, Washington, Nevada, and British Columbia from the late 1800s to October 2021 from iNaturalist (*22)* and the Western Monarch Milkweed Mapper (*23)*; these observations included latitude, longitude, and day of year of observation. Most analyses in this paper are based on data only through December 2020. We added supplemental analyses of data from January-October 2021 to check patterns during the most recent year (Extended Data Figure 3, and see last paragraph of main text). There are resident populations of monarch butterflies in Southern California and southern Nevada.

Therefore, to evaluate breeding season range expansion, we focused on Northern California and northern Nevada. Specifically, we removed all observations south of the line drawn by connecting the locations (-120.63 lat, 34.75 lon) and (-114.02 lat, 38.49 lon). We also excluded observations less than 10 kilometers from the coast, as some fraction of individuals remain on the coast year-round. (The specific distance cutoff used for exclusion did not matter; see "Sensitivity analysis" and Extended Data Fig. 2, below). We removed duplicate observations (same date, and latitude and longitude each within 1/1000 degrees of each other), and removed obvious outliers based on expert opinion (36 outliers total). Criteria for outliers included observations at sea, outside of the known monarch butterfly range, observations in Washington and Oregon in December, and observations based on observer's childhood memories; the 36 outliers can be found in the supplements in `2_data_wrangling/outliers-gbif.csv`, `2_data_wrangling/outliers-wmmm.csv`. For each of the remaining 4489 observations, we calculated the great circle distance ("as the crow flies") to the nearest overwintering sites, using the 185 overwintering sites of (*5)* and the function distCosine() from the R package **geosphere** (*39)*. For this analysis, we used summer 2018 as the start of the "current" (low population) era, because the low abundance started in spring 2018 (as shown by (*6)*). Analyses of 2021 data (Extended Data Fig. 3) use the same methods and data sources, but use only data through October 27, 2021 (592 points).

Plots of observations based on day of year and distance from the nearest overwintering sites showed a roughly symmetrical, hump-shaped distribution that could be approximated by a Gaussian curve (e.g. Fig. 3B). In (*40)* we show how Gaussian curves can be fit with linear models; we combine this approach with the rq() function from the **quantreg** package, which fits a linear model with quantile regression (*41)*. We used the 0.9 quantile to represent the outer

boundary of the monarch range; this captures the expansion of monarchs into their summer breeding range while still being robust to outliers (but the specific quantile chosen did not matter: see below). We used the methods of (*40)* to calculate derived metrics including the maximum distance and day of maximum distance; we used similar algebra to calculate the day each fitted curve reached a specified distance (e.g. Fig. 3D-E). We estimated confidence intervals using bootstrapping as implemented in the **msm** R package (*28)*. We did not have sufficient data to fit most years on their own (but see Extended Data Fig. 3 for yearly fits of 2015-2020), so we aggregated observations to the historic, recent past, and current eras. All calculations of timing are based on day of year (0-366); for readability we present our results as month and day for a non-leap-year.

Sensitivity analysis

To confirm that our results did not depend on specific model-fitting decisions, we repeated this analysis with each of the following changes: (a) defining the monarch range by the 0.8, 0.7, 0.6, and 0.5 quantiles, or (b) changing the distance from coast below which we excluded points to 0.1 km, and then 40 km. Estimates changed, but the same qualitative patterns remained (Extended Data Fig. 2, Table S1).

We observed apparent streaks in the raw data when plotting distance by day of year (Fig. 3B, Extended Data Fig. 4). The highly overrepresented distances may reflect repeated sampling of a popular location. To ensure these streaks were not driving observed patterns, we generated simulated data sets by randomly subsampled our data such that we never had more than 1 data point in each 1km distance from the overwintering sites (e.g. each 1-km bin in Extended Data Fig. 4) for each era (Extended Data Fig. 5). This sampling procedure generated simulated data sets with 1276 observations instead of 4492. We repeated this process 5000 times and carried out

our previous analysis on each of these simulated datasets. Specific values changed somewhat, but we find qualitatively similar results to our analysis of the full data set.

Data availability: All custom scripts and data that support the findings of this study will be deposited to Dryad prior to final publication.

Methods References

24. R Core Team, R: A Language and Environment for Statistical Computing (2021), (available at https://www.R-project.org/).

25. E. E. Holmes, E. J. Ward, K. Wills, MARSS: Multivariate autoregressive state-space models for analyzing time-series data. The R Journal. 4 (2012), p. 30.

26. A. Rohatgi, Webplotdigitizer: Version 4.5 (2021), (https://automeris.io/WebPlotDigitizer).

27. B. K. Williams, J. D. Nichols, M. J. Conroy, Analysis and Management of Animal Populations (Academic Press, 2002)

28. C. Jackson, Multi-State Models for Panel Data: The msm Package for R. Journal of Statistical Software, Articles. 38, 1–28 (2011).

29. H. Wells, P. H. Wells, The monarch butterfly: A review. Bulletin of the Southern California Academy of Sciences. 91, 1–25 (1992).

30. P. M. Tuskes, L. P. Brower, Overwintering ecology of the monarch butterfly, *Danaus plexippus* L., in California. Ecol. Entomol. 3, 141–153 (1978). doi: 10.1111/j.1365-2311.1978.tb00912.x

31. S. B. Chaplin, P. H. Wells, Energy reserves and metabolic expenditures of monarch butterflies overwintering in southern California. Ecol. Entomol. 7, 249–256 (1982). doi: 10.1111/j.1365-2311.1982.tb00664.x

32. K. L. H. Leong, E. O'Brien, K. Lowerisen, M. Colleran, Mating activity and status of overwintering monarch butterflies (Lepidoptera: Danaidae) in Central California. Ann. Entomol. Soc. Am. 88, 45–50 (1995). doi: 10.1093/aesa/88.1.45

33. G. Beall, Seasonal variation in sex proportion and wing length in the migrant butterfly, *Danaus plexippus* l. (Lep. Danaidae). Trans. R. Entomol. Soc. Lond. 97, 337–353 (1946). doi: 10.1111/j.1365-2311.1946.tb00268.x

34. T. Van Hook, in 1997 North American conference on the monarch butterfly (Commission for Environmental Cooperation, 1999; p. 101.

35. K. H. L. Leong, M. A. Yoshimura, C. Williams, Adaptive significance of previously mated monarch butterfly females (*Danaus plexippus* (Linneaus)) overwintering at a California winter site. lepi. 66, 205–210 (2012). doi: 10.18473/lepi.v66i4.a3

36. S. Jackman, pscl: Classes and Methods for R Developed in the Political Science Computational Laboratory (2020), (available at https://github.com/atahk/pscl/).

37. A. Zeileis, C. Kleiber, S. Jackman, Regression Models for Count Data in R. J. Stat. Softw. 27, 1–25 (2008).

38. H. Dingle, M. P. Zalucki, W. A. Rochester, T. Armijo-Prewitt, Distribution of the monarch butterfly, *Danaus plexippus* (L.) (Lepidoptera: Nymphalidae), in western North

America. Biol. J. Linn. Soc. Lond. 85, 491–500 (2005). doi: 10.1111/j.1095-8312.2005.00512.x

39. R. J. Hijmans, Geosphere: Spherical Trigonometry. 2016. R package version 1.5--5 (2019).

40. C. B. Edwards, E. E. Crone, Estimating abundance and phenology from transect count data with GLMs. Oikos (2021). doi: 10.1111/oik.08368.

41. R. Koenker, quantreg: Quantile Regression (2021), (available at https://CRAN.R-project.org/package=quantreg).

42. K. S. Oberhauser, Effects of spermatophores on male and female monarch butterfly reproductive success. Behav. Ecol. Sociobiol. 25, 237–246 (1989). doi: 10.1007/BF00300049

43. K. S. Oberhauser, Fecundity, lifespan and egg mass in butterflies: effects of male-derived nutrients and female size. Funct. Ecol. 11, 166–175 (1997). doi: 10.1046/j.1365-2435.1997.00074.x

Acknowledgments:

Leone Brown, Norah Warchola, and Chelsea Thomas assisted with the field surveys and extraction of previously published results; Emma Pelton and Stephanie McKnight provided guidance and insight in working with Xerces data. California State Parks, California Department of Fish and Game and USFWS were all important in securing permits to work with monarch butterflies at Pismo Beach State Park. California State Parks generously provided use of their greenhouse to conduct studies on reproductive biology of female monarchs at Pismo Beach, including Danielle Bronson, Stephanie Little and Ronnie Glick. Cheryl Powers, a docent volunteering at the Pismo Beach site, generously opened her home to us to support lodging needs by staff throughout February 2019, and Shore Cliff Hotel donated additional lodging during the peak activity period. We are grateful to Marm Kilpatrick and Sarina Jepsen for discussions during planning and interpretation of data. Funding for this work was contributed by CREOi (Conservation Research Education and Opportunities International), WSU Vancouver Fund for Ecology and Conservation of Northwest Butterflies and Their Habitats as well as private donors to WSU and UC Santa Cruz, and the National Science Foundation DEB 1920834.

Author contributions:

Conceptualization: CBE, CBS, EEC

Data Curation: CBE, CBS, EEC

Formal Analysis: CBE

Funding acquisition: CBS, EEC

Investigation: CBS, EEC

Methodology: CBE, EEC

Project administration: EEC

Software: CBE

Supervision: CBS, EEC

Visualization: CBE

Writing – original draft: CBE

Writing – review & editing: CBE, CBS, EEC

Competing interests: Authors declare they have no competing interests.

Supplemental Information is available for this paper. Correspondences and requests for materials should be addressed to CBE.

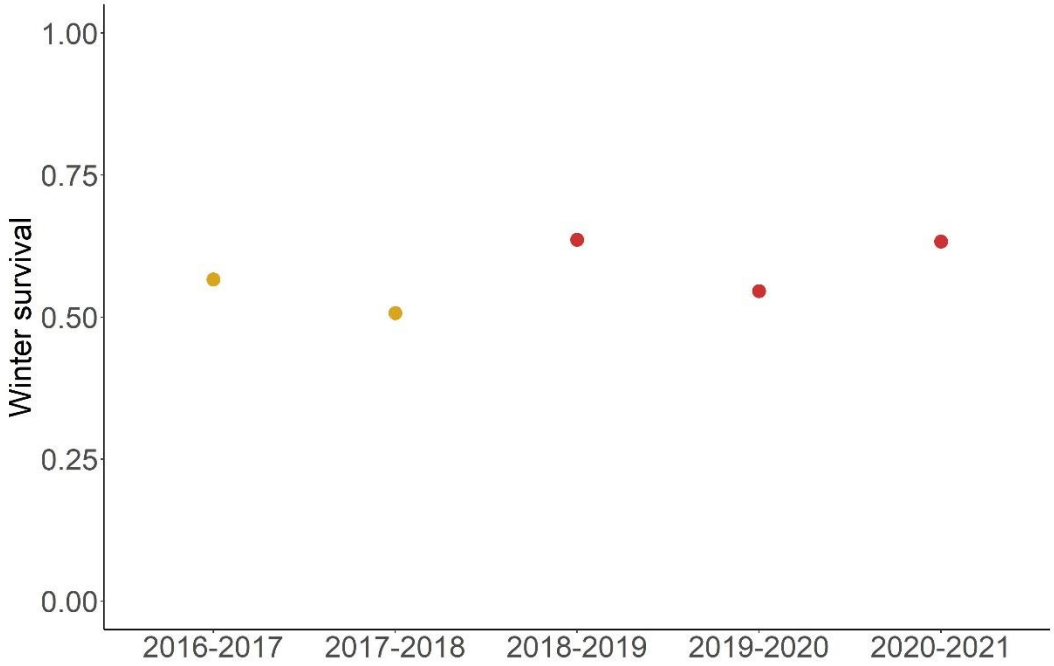

Extended Data Fig. 1 | Yearly point estimates for 6-week winter survival are similar across recent past (yellow) and current (red) eras. As Fig. 2A in the main text, except estimated on a yearly basis rather than aggregated to the era level.

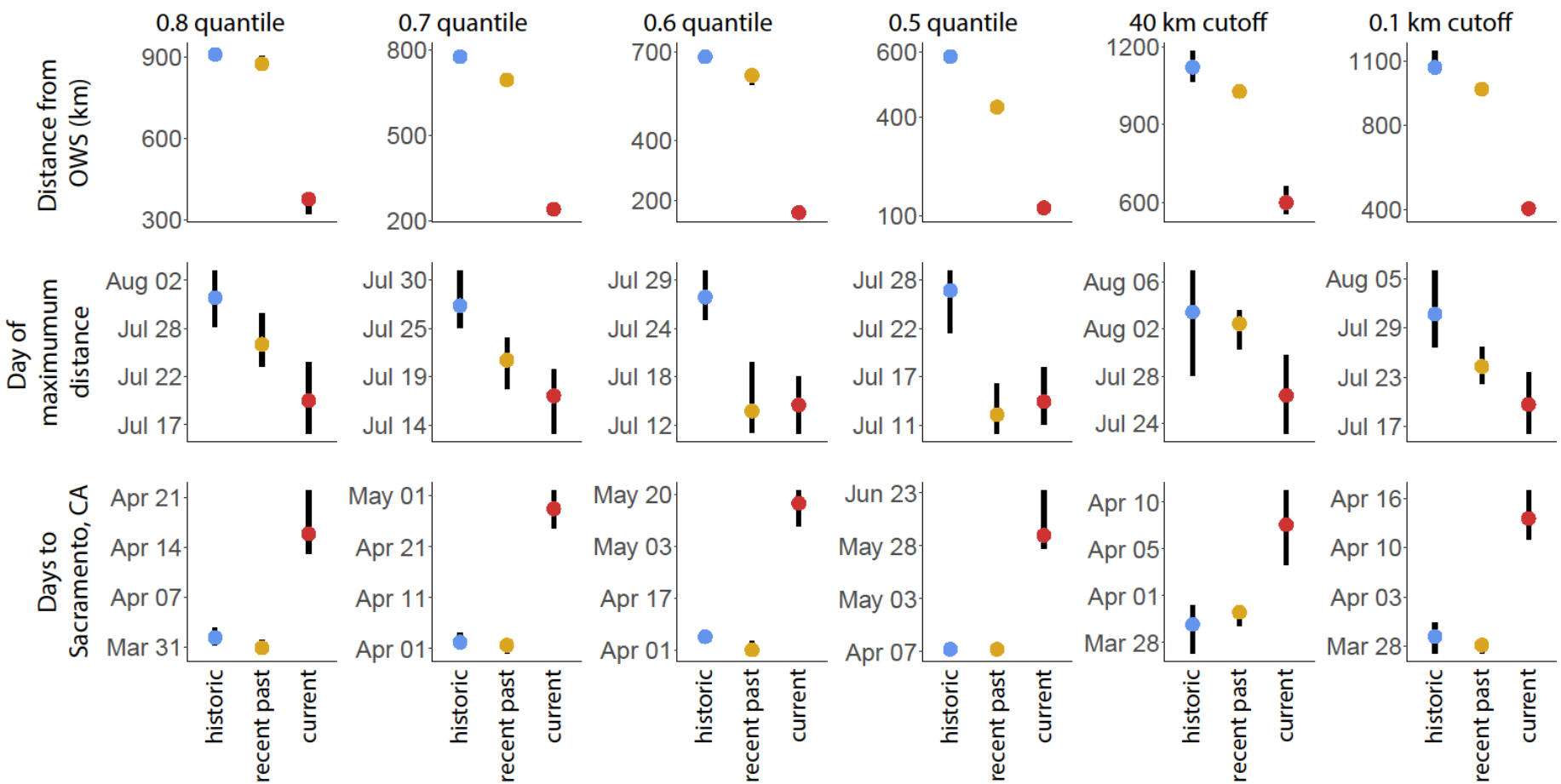

Extended Data Fig. 2 | Varying quantile choices, cutoff thresholds from the coast does not qualitatively change results. We repeated the analysis of the main text (Fig. 2F, Fig. 3C-D) using different parameterizations of the model. Maximum distance from overwintering sites in kilometers (**row 1**), day of maximum distance (**row 2**), and first day when the fitted curve exceeds 100 km

(**row 3**) show similar patterns to the analyses from the main text when fitted using 0.8, 0.7, 0.6, and 0.5 quantiles (**columns 1-4)** (main text uses 0.9), and when excluding data within 40 km (**column 5**) or 0.1 km (**column 6**) of the coast (main text uses 10km). Note the differing scales on the y axis. Bars show 84% CI calculated from 1000 bootstraps.

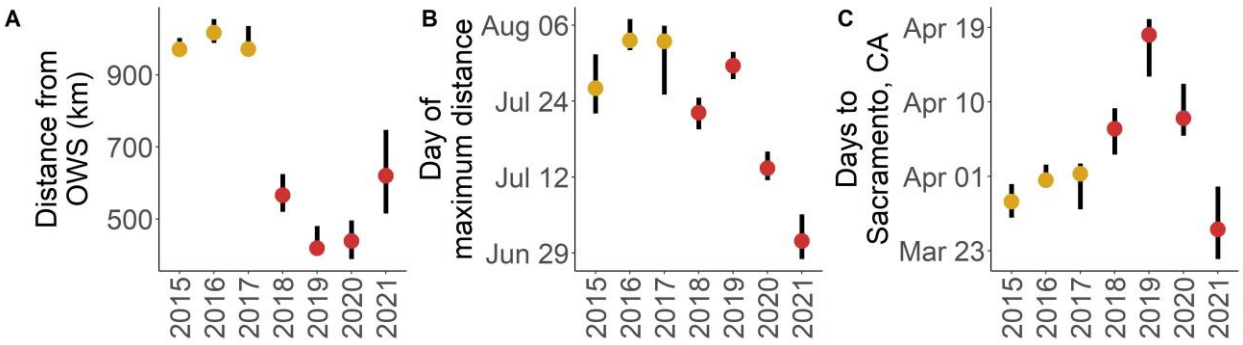

Extended Data Fig. 3 | Patterns largely hold when analysis is repeated using individual years. There was generally insufficient data to fit the 0.9 quantile on a yearly basis, but a recent surge in monarch observations allows us to fit each year of 2015-2021 separately. (A-C) Breeding range measures analogous to Fig. 2F, Fig. 3C-D. Bars show 84% CI. (A) and (C) show clear differences between eras that reflect the patterns reported in the main text, although year to year variation from 2018-2020 suggest that monarchs had particularly late phenology in 2019. Note that 2021 estimates were fit using observations through October 27, 2021; these preliminary estimates show that despite the dramatic population growth of 2021, the spatial Allee effect still occurred.

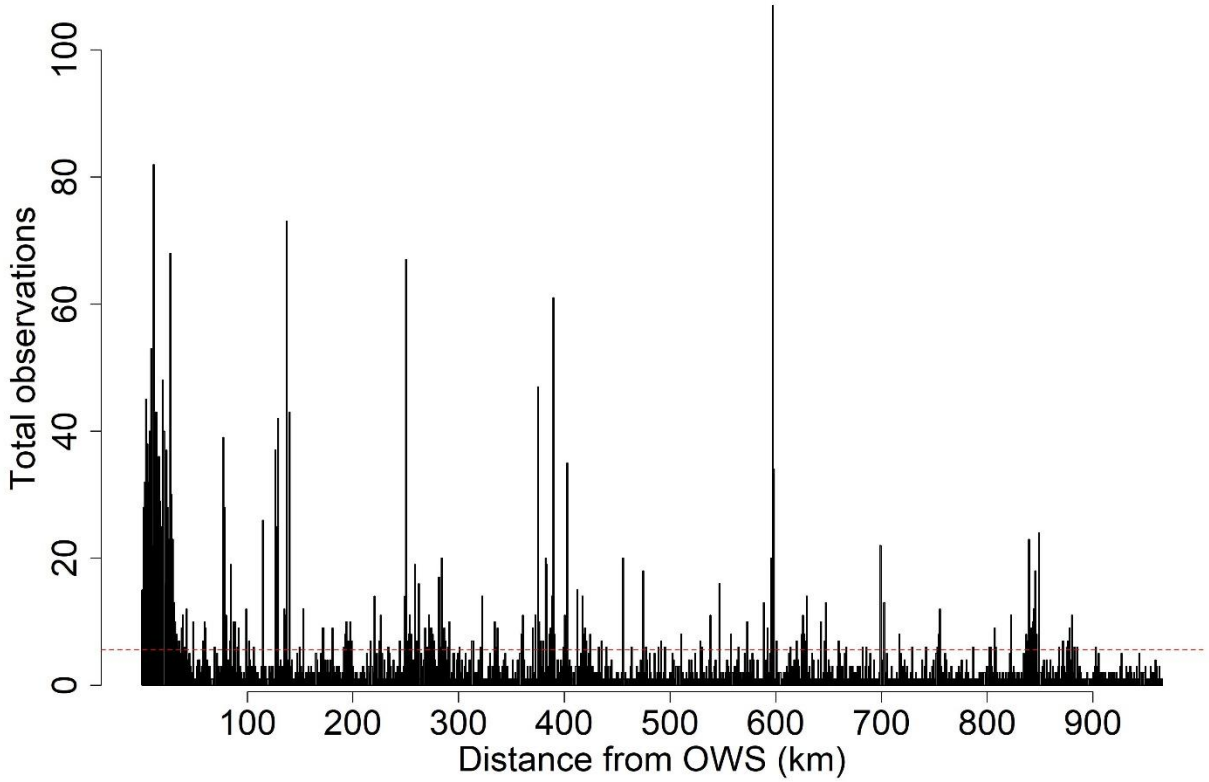

Extended Data Fig. 4 | Observations are not distributed evenly across distances from overwintering sites. Each bar represents the total number of observations in an individual 1-kilometer bin. Dashed red line shows the average across all bins; some bins have 10-20x this average representation.

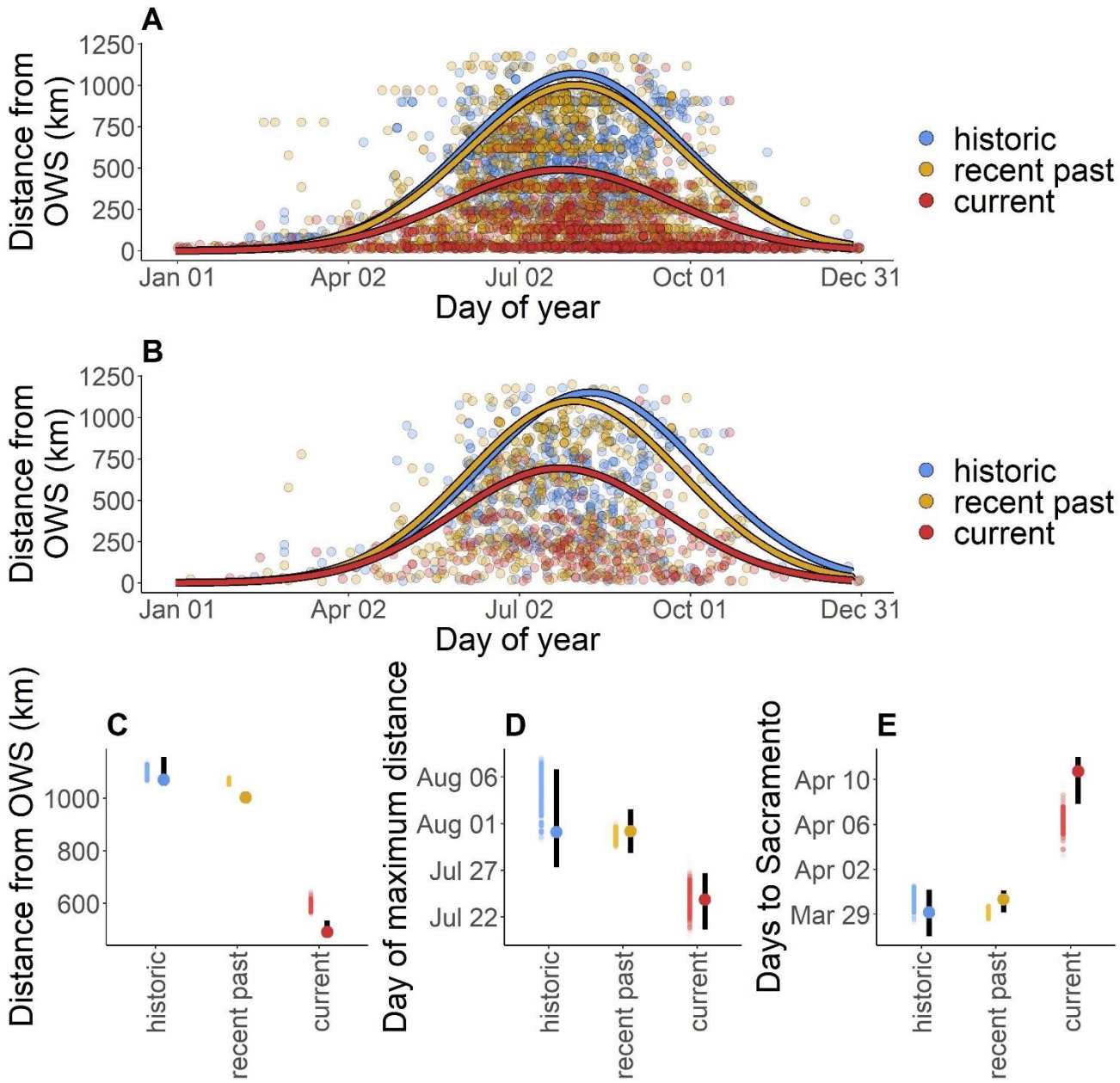

Extended Data Fig. 5 | Data subsetted to reduce streakiness shows qualitatively similar results to estimates using the complete data sets. (**A**) Curves fitted to the complete data set, as in main text (for comparison). (**B**) Curves fitted to a subset of the data, generated by randomly subsampling such that there is only one observation per era per kilometer distance from the overwintering site. This reduces the horizontal patterns in the data visible in (A). (**C-E**)

Comparison of point estimates from 5000 iterations of subsampling demonstrated in (B) (semi-transparent points, left) with the point estimate and 84% CI obtained from fitting complete data set as in the main text (right, solid point and black bar). We see qualitatively – and often quantitatively – similar patterns with the reduced data sets.

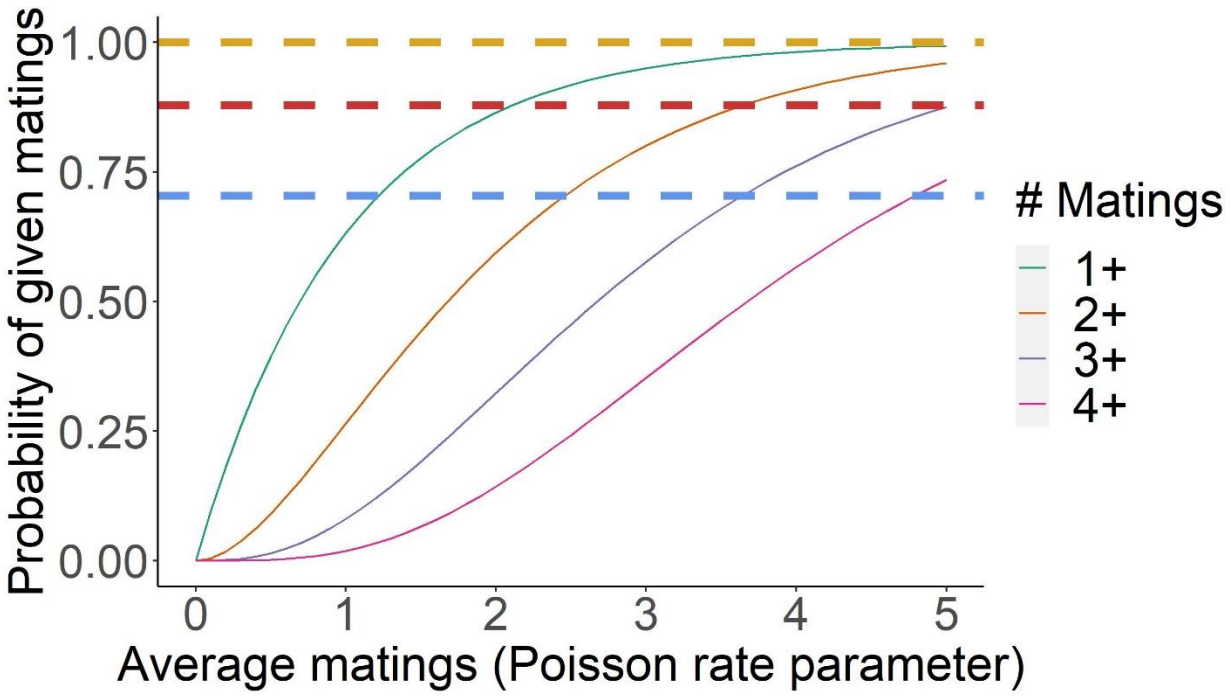

Extended Data Fig. 6 | Changes in mating rates impact multiple-mating proportions more rapidly than overall fraction of mated individuals. Plots of calculated mating success assuming Poisson-distributed mating numbers (see Supplemental Information). Dashed blue, yellow, and red lines show estimated probability of one or more matings for the historic, recent past, and current eras (i.e. Fig. 2D). Solid curves show the fraction of individuals with at least 1, 2, 3, or 4 matings assuming Poisson-distributed matings. Across the span of average matings implied by observed mating success in different eras (~1.2 to >5), there is a small change in the fraction of individuals mated at least once, but substantial changes in the number of individuals mated at least 2, 3 or 4 times.

Extended Data Table 1 | Estimates and 95% confidence intervals when using alternate quantile choice, cutoff threshold from coast. "Variant" column describes either the new quantile or new cutoff threshold (analysis in main text used the 0.9 quantile and a 10 km cutoff); estimates and bootstrapped 95% CIs for day of peak distance, maximum distance, and day of year the quantile reached 100 km were calculated as in the main text but using the new quantile or cutoff. CIs were estimated from 1000 bootstraps.

Variant	Era	Day of peak distance			Maximum distance from OWS			Days to Sacramento		
		Estimate	2.5% CI	97.5% CI	Estimate	2.5% CI	97.5% CI	Estimate	2.5% CI	97.5% CI
0.8 quantile	historic	212.50	209.39	215.37	910.66	895.71	921.60	91.54	90.47	92.88
0.8 quantile	recent past	207.46	205.01	210.80	875.79	856.63	904.71	90.08	89.25	91.25
0.8 quantile	current	201.35	197.74	205.49	375.30	319.21	395.37	106.29	103.51	112.38
0.7 quantile	historic	208.77	206.28	212.61	775.05	760.12	794.00	92.98	91.71	94.79
0.7 quantile	recent past	202.67	199.53	205.12	694.48	684.94	718.45	92.41	90.72	93.39
0.7 quantile	current	198.69	194.42	201.59	241.20	223.75	260.24	119.14	115.42	122.65
0.6 quantile	historic	208.83	206.25	211.84	682.91	666.86	701.19	95.56	94.11	97.05
0.6 quantile	recent past	195.62	193.10	201.24	620.12	588.48	626.18	91.45	90.26	94.32
0.6 quantile	current	196.33	192.95	199.61	158.55	152.83	175.01	137.19	130.00	141.07
0.5 quantile	historic	208.25	203.28	210.52	586.22	567.02	601.83	98.59	96.40	99.84
0.5 quantile	recent past	193.59	191.30	197.28	431.74	415.61	449.00	98.58	97.12	100.95
0.5 quantile	current	195.11	192.44	199.19	124.14	104.32	131.70	153.91	147.52	175.48
40km cutoff	historic	215.69	209.90	219.40	1120.75	1064.50	1181.43	89.19	86.58	90.83
40km cutoff	recent past	214.61	212.30	215.84	1027.12	1014.26	1051.21	90.26	89.02	90.83
40km cutoff	current	208.10	204.59	211.76	598.95	554.13	659.91	98.04	94.46	101.05
0.1km cutoff	historic	212.48	208.31	218.04	1070.22	1040.00	1145.58	88.65	86.44	90.49
0.1km cutoff	recent past	205.74	203.49	208.27	967.87	955.41	989.49	87.55	86.55	88.46
0.1km cutoff	current	200.85	197.03	204.97	405.93	379.12	424.75	103.89	101.22	107.46

Movie S1: Western monarch yearly range expansion reaches half the distance and takes up to two months longer since the population fell below the hypothesized Allee effect threshold. Top: plots of observations separated by era (Historic = 20th century, Recent past = 2000-2017, Current = 2018-2020). Colored circles represent observations in the last 7 days; smaller white diamonds act as placeholders to identify locations of earlier observations. Note the exclusion of AZ and southern regions of CA and NV to avoid resident populations. Only points at least 10 kilometers from overwintering sites are plotted. Bottom: the same observations plotted by day of year and distance from the nearest overwintering sites; curves show Gaussian curves fit to the 0.9 quantile of observations for each era, representing the yearly expansion into the summer breeding range.